Marcus T. Cicerone,[1] Joy P. Dunkers,[1] and Newell R. Washburn[1]

Towards *In-Situ* Monitoring of Cell Growth in Tissue Engineering Scaffolds: High Resolution Optical Techniques

---

Reference: Cicerone, M.T., Dunkers, J.P., and Washburn, N.R., "**Towards *In-Situ* Monitoring of Cell Growth in Tissue Engineering Scaffolds: High Resolution Optical Techniques,"** *Tissue Engineered Medical Products (TEMPs) ASTM STP 1452*, G.L. Picciolo and E. Schutte, Eds., ASTM International, West Conshohocken, PA, 2003.

Abstract: Inability to obtain cellular-level information about progress of cell growth in tissue-engineering (TE) scaffolds is a pervasive problem. We demonstrate that a confocal microscope with two collinear contrast mechanisms, optical coherence, and fluorescence, can be used to perform non-destructive imaging of a polymer TE scaffold containing osteoblasts. We show that the combination of the techniques shows promise for *in situ* measurements of cell growth in a bioreactor, even for highly opaque TE scaffolds.

Keywords: coherence microscopy, fluorescence microscopy, morphology, OCT, tissue engineering scaffold

Introduction

It is generally understood that a complex interaction of many variables influences the success of cell infiltration, proliferation, and differentiation within a tissue scaffold (TS). One characteristic that has a large influence on the development of functioning tissue is the three-dimensional (3D) morphology of the scaffold itself [1,2].

---

[1] Research Scientists, Polymers Division, National Institute of Standards and Technology, 100 Bureau Drive, Mail Stop 8543, Gaithersburg, MD 20899-8543.

Quantification of morphological characteristics of the pores, such as volume, size distribution, connectivity, tortuosity, local curvature and composition, and comparison of those quantities with local cell viability will undoubtedly play an important role understanding the rich interaction between scaffold and cell.

A non-invasive method for scaffold characterization and, ideally, simultaneous cell monitoring, is needed. X-ray computed micro-tomography has been used to yield 3D images of biomaterials at a resolution of 14 μm, [3] and more recently, commercial instruments are available with resolution of (2 to 3) μm, but while this method is innocuous to the scaffold, it has the disadvantage of being potentially damaging to biological tissue, so that *in-situ* imaging is not feasible. NMR [4] has also been used for 3D imaging of biomaterials and tissues, but spatial resolution attainable by NMR methods is typically about 10 μm; insufficient for imaging at the cellular level. Confocal microscopy can give the desired spatial resolution, and is used extensively for cellular imaging in optically "clean" samples. Some work has been reported on scaffold characterization using laser scanning confocal microscopy (LSCM) [5,6], but the image depth is limited to ≈ 80 μm in more opaque systems, such as many TE scaffolds, due to large background signals from scattered light.

Optical coherence tomography (OCT) is a photon time-of-flight method that has both excellent background rejection capability against light scattered out-of-plane, good dynamic range (> 100 dB), and good sensitivity (≈ 1 pW reflected light), making it ideal for obtaining image data deep in highly scattering media. However, without an expensive ultra-broadband light source [7], OCT generally does not give spatial resolution at the ≈ 1 μm level that is desirable for monitoring cells and obtaining structural information of the scaffold. Izatt et al. [8] demonstrated that when an OCT instrument is configured with confocal optics, the instrument response, or point spread function (PSF) is a product of the OCT and confocal PSFs. Thus, a confocal OCT, or optical coherence microscope (OCM) gives the background rejection, sensitivity, and dynamic range of an optical coherence tomography instrument, and also excellent spatial resolution inherent in a confocal microscope. We have taken the additional step of implementing a fluorescence detection channel that is collinear with the OCM channel. In this way we will be able to obtain structural information from the OCM simultaneously with functional information about, e.g. labeled cells, from the fluorescence channel. Beaureparie et al. have implemented a similar marriage previously [9]. They used 830 nm light from a femtosecond laser system to excite two photon fluorescence and simultaneously collected a coherence signal. The system we describe below is significantly less expensive.

In this work we report on nondestructive imaging of a polymeric TE scaffold, demonstrating the improvement in resolution with OCM, as compared to OCT. We also present preliminary data to show the applicability of the OCM / fluorescence combination to *in-situ* cell monitoring, even deep within a TE scaffold.

Experimental

Scaffold Preparation

Poly(ε-caprolactone) (PCL) is blended with poly(ethylene oxide) (PEO) in a twin-screw extruder to form a bicontinuous, two-phase material with micrometer-sized domains. In this work, PCL and PEO were mixed in equal weights. Selective dissolution of the PEO with water results in a porous material, the characteristic pore size of the TE scaffold is controlled by annealing and can reach in excess of 100 μm. The scaffolds in this work were annealed at 75 ^{o}C for times in the range of (20 to 30) min. A more detailed description of scaffold preparation is provided elsewhere [10]. The scaffold was immersed in an index matching fluid prior to imaging.

Microscopy Optics and Instrumentation

Figure 1 shows a schematic of our OCM / fluorescence setup. The OCM system consists of a superluminescent diode (SLD) centered at 1.31 μm, in the near infrared (NIR), with a bandwidth of 70 nm (AFC, Hull, Quebec, Canada).[2] The detection system is a fiber-optic optical coherence domain reflectometer built by Optiphase (Van Nuys, CA). The reflectometer is capable of distinguishing reflections with s and p polarization, but in this work, we are monitoring only s reflections. The NIR light is transported by a single mode, polarization-maintaining fiber (0.16 NA), and is launched into a bulk optic system via a 0.55 NA collimating lens. The light then passes through a variable neutral density filter and a cold mirror. A 3:1 expanding

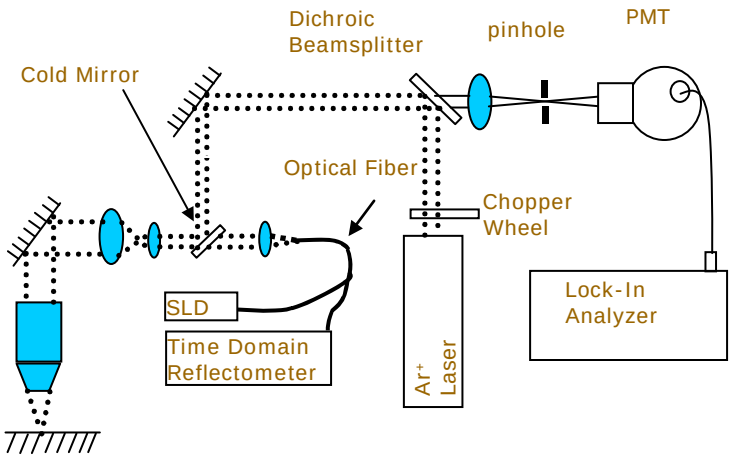

Figure 1 - Experimental configuration of collinear OCM and confocal fluorescence instruments. See text for explanation.

[2] Identification of a commercial product is made only to facilitate experimental reproducibility and to adequately describe experimental procedure. In no case does it imply endorsement by NIST or imply that it is necessarily the best product for the experimental procedure.

telescope is employed to fill the aperture of the objective, an EpiPlan –NEOFLUAR 100X 1.3 NA oil-immersion objective (Zeiss, Germany). The objective has a working distance of 370μm. Reflected light is returned to the single mode fiber, which acts as a confocal aperture for the detection system. The return light has essentially the same ray characteristics as the light delivered (beam diameters, etc.); thus, since the emission and collection aperture are the same, the collection aperture is fixed at 1 Airy unit (AU).

The reference arm of the interferometer is driven by piezoelectric modulators at 300 Hz and filtered at a Doppler frequency of 705 kHz. The dynamic range of the system is 110 dB. In the absence of the high NA objective, (i.e., in OCT mode), this instrument is capable of 19 μm axial resolution, which is slightly degraded from the 12 μm theoretical value for a 70 nm bandwidth source due to group dispersion velocity mismatch in the sample and reference arms. The theoretical values for transverse and axial spatial resolution of the confocal OCM configuration are 0.51 μm and 1.4 μm respectively. The theoretical axial resolution is obtained as the FWHM of the product of the point spread functions of the OCT (Gaussian, with FWHM of 19 μm), and the confocal geometry (Lorentzian with FWHM of 1.5 μm).

A first-surface mirror was moved axially through the focus of the beam, and the OCM response was measured as a function of the axial position of the mirror. The axial resolution of the system was determined to be 1.5±0.3 μm (FWHM of the response function), which is in accord with the theoretical value for a detection pinhole of 1 Airy unit (AU).

Figure 1 also shows the confocal fluorescence system, which is comprised of an air-cooled Omnichrome argon ion laser (Melles Griot, Carlsbad, CA). The 488 nm laser light is sent through a bandpass filter, a dichroic beam splitter, and several turning mirrors before reaching a cold mirror where it becomes collinear with the NIR beam. The fluorescence signal propagates back to the dichroic beam splitter where the excitation line is filtered out. Confocal gating of the fluorescence signal is accomplished by passing the collected light through a 10 μm pinhole that was placed at focus of a 0.15 NA objective. The excitation light was chopped at 1.5 kHz, and the fluorescence signal was detected using a photo-multiplier tube (Oriel, Stratford, CT) and lock-in amplifier (Perkin Elmer, Freemont, CA).

The focal points of the 488 nm

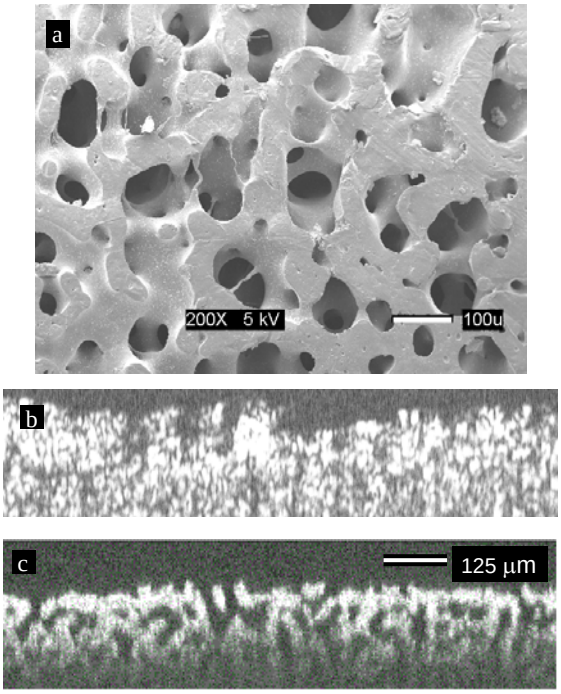

Figure 2 - a) SEM of PCL Scaffold, annealed for 20 min at 75 ^{o}C. b) and c) OCT and OCM images (respectively) taken on a similar scaffold to that in a). Imaging conditions for SEM, OCT, and OCM are given in the text.

and NIR beams are separated by (5.8 ± 0.1) μm,[3] with the visible light being focused closer to the objective. This is due to chromatic aberration of the objective. It could be corrected by using a reflective objective, or by delivering a slightly converging NIR beam or slightly diverging visible beam to the objective.

Two-dimensional imaging is performed simultaneously for the OCM and fluorescence channels by repeating a process of scanning the sample in the x direction and subsequently stepping in the y direction. The scanning and stepping are accomplished using motorized stages (Newport, Irvine, CA). After each x-y scan, the sample is moved in the z direction by a motorized stage with a maximum resolution of 100 nm (ASI Inc., Eugene, Oregon). The x-y stages were not designed for high-resolution work; they are specified by the manufacturer to give resolution of 1 μm and repeatability of 5 μm. Our experimental lateral resolution depends on repeatability, and is limited to 5 μm in all OCM / fluorescence images presented here by the x-y stage performance. Experimental axial resolution is limited by the optical arrangement, and is the same as is specified above.

Results and Discussion

Figure 2 shows images of PCL TE scaffolds obtained by SEM, OCT and OCM. Other than contrast scaling adjustments, no post-processing image manipulation routines have been applied. Image a) is an SEM image from a PCL scaffold that was annealed for 20 min at 75 °C. In preparation for data acquisition, the TS was rinsed with methanol, dried under vacuum, and sputter-coated with gold. The SEM image was obtained with a Jeol JL-5300 electron tomograph operating at 5 kV and 50 μA. Images b) and c) are cross-sectional images of PCL scaffolds that were annealed for 30 min at 75 °C, obtained with OCT and OCM respectively. In these images, the white pixels represent volumes from which reflection was detected (i.e. occupied by scaffold matrix material). One sees immediately that without further image manipulation it is impossible to distinguish clearly between pore and matrix from the OCT data, however, the contrast obtained with OCM is sufficient that this distinction can be made easily. The apparent loss of sensitivity at depths greater than 150 μm

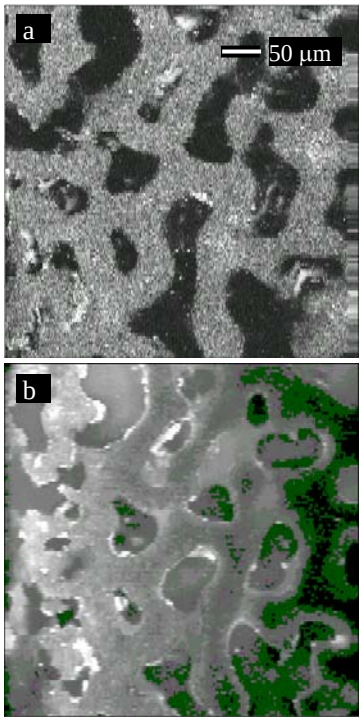

Figure 3 - Dual mode imaging of a PCL scaffold cultured with fluorescently stained osteoblasts. The images were acquired near the scaffold surface. a) confocal OCM image. b) confocal fluorescence image.

[3] All statements of standard uncertainty quoted herein are ± 1 standard deviation.

below the scaffold surface in image c) is due to a sub-optimal optical configuration in place at the time that this data was acquired. Also, due to the optical configuration available at the time, the axial and lateral optical resolution of image c) are 6 μm and 1.5 μm respectively. Better optical quality is obtained and displayed in the images of Figures 3 and 4.

There appears to be a difference in the pore distribution size between images a) and c) in Figure 2; in particular, the pores seem to be smaller in the latter. This apparent difference probably reflects a real difference in the pore sizes. The two scaffolds represented here were made with different batches of PCL. While both batches had a nominal weight average molecular weight of 80 000, the batch from which the scaffold in image a) was made seems to have a slightly lower average molecular weight that the other. This supposition is based on the relative processing characteristics of the two batches, and was not tested quantitatively, but is consistent with the difference in average pore size we see.

Figure 3 shows confocal OCM and fluorescence images from the same TE scaffold in the top and bottom panels, respectively. This scaffold was seeded with primary chick osteoblasts and incubated for six weeks. The cells were then fixed and stained with eosin, so that they could be visualized by fluorescence microscopy.

The dark areas in the OCM image represent pores, and the lighter areas are the scaffold matrix. With the improved spatial resolution that we attain with OCM over OCT, we are able to obtain clear scaffold images with good spatial resolution. It was not our expectation that OCM would give much contrast between the cells and the matrix, but the highly reflective (white) areas in this image appear to be due to cell colonies. This is supported by the fluorescence image (lower panel). The bright areas here represent groups of cells. We notice that the cells are adhered to the scaffold walls, as expected, and that there does not seem to be any strong preference for either high local curvature or flatter surfaces, although these images have not been analyzed quantitatively. We note that the fluorescence data were obtained very near the top of the scaffold, and that the gradual transition from high to low background as you go from left to right in the image is due to a slight tilt of the scaffold with respect to the image plane. In the left side of the image, some intensity was probably due to cells found on the top surface of the scaffold.

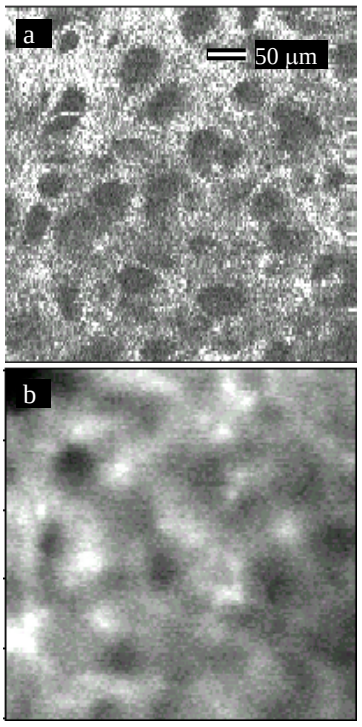

Figure 4 - Dual mode imaging of a PCL scaffold, stained with acridine orange. The images were acquired 180 μm from scaffold surface. a) confocal OCM image. b) confocal fluorescence image.

Differences in the morphology of the scaffold are apparent between the two images in Figure 3. These differences

originate from the fact that image planes are separated by roughly 6 μm, with the OCM image being deeper into the sample, as indicated above. Due to this separation, one gets a sense for the local 3D structure by comparing the differences between the images. We also note that we did not find appreciable cell population in the scaffold imaged in Figure 3. This may have been due to poor perfusion of nutrient, or a "skin" which sometimes forms near the surface during preparation of the scaffold.

Ultimately, one would like to image cells deep in the scaffold, noninvasively, and with high resolution. This is particularly difficult when the scaffold material is highly scattering, as is the case for the polycrystalline PCL scaffolds imaged here; data quality will gradually degrade as one attempts to image deeper into the scaffold. However, due to the background rejection capability of OCM, we are able to obtain structural information even 180 μm into the scaffold, when steps are taken to ameliorate the mismatch of refractive index between the bath and the PCL. We observe that when index-matching oil ($n_D = 1.563$) is used as the bath, imaging with the OCM can be accomplished down to about (175 to 250) μm. If an aqueous solution of ≈ 0.40 mass fraction glycerol is used as the index-matching bath, the imaging range does not suffer significantly and this bath is not likely to be harmful to biological tissues for brief exposure. At present we can scan a single OCM frame in (10 to 15) minutes, so a reasonable volumetric image can be acquired in approximately 1 day. The scan rate could be increased by a factor of five or ten with appropriate scanning stages.

Figure 4 was obtained by staining the surface of the scaffold with acridine orange from a methanol solution, then imbibing the scaffold with immersion oil. The top image was obtained with OCM, and though the contrast suffers with respect to the image taken at the surface, the resolution is still fairly good. Thus, reliable structural information can still be obtained. No cells were seeded into this scaffold, however it is possible that they would give enhanced reflectivity here as they did in the top panel of Figure 3. The bottom image of Figure 4 is a confocal fluorescence image. The spatial resolution is poor, but we are still able to obtain some contrast. This means that we could detect the presence of fluorescently labeled cells, whether stained, or engineered to express a fluorescent protein. Thus, by combining the information obtained by confocal OCM with that obtained by confocal fluorescence, we expect to be able to monitor progress of cell growth, even deep within a TE scaffold. This will be facilitated if we find enhanced reflectivity at the cell surface of NIR light such as that seen in Figure 3 a.

Conclusions

We have obtained high fidelity images of tissue engineering scaffolds using the strengths of two complimentary contrast mechanisms, optical coherence and fluorescence, in a confocal microscope. The coherence technique allows us to obtain images with good spatial resolution, even deep into the scaffold material. Fluorescence detection allows us to detect fluorescent signal equally far into the sample, but with significantly less spatial resolution. When used in parallel, these contrast mechanisms allow us to detect the presence and / or continuing viability of cells that are stained or expressing fluorescent protein deep within a TE scaffold, and to correlate their growth

with local and surrounding scaffold morphology. In principle, such information can be obtained nondestructively, and *in situ*, such that information on a single sample can be obtained throughout the tissue growth process.

References

[1] Ma,T., Li, Y., Yang, S.-T., and Kniss, D., "Effects of Pore Size in 3-D Fibrous Matrix on Human Trophoblast Tissue Development," *Biotechnology and Bioengineering*, Vol. 70, No. 6., 2000, pp. 608-618.

[2] Dillon, G., Yu, X., Sridharan, A., Ranieri, J., and Bellamkonda, R., "The Influence of Physical Structure and Charge on Neurite Extension in a 3D Hydrogel Scaffold," *Journal of. Biomaterial. Science: Polymer Edition.*, Vol. 9, No. 10, 1998, pp. 1049-1069.

[3] Muller, R., Matter, S., Newenschwander, P., Suter, U.W., and Ruegsegger, P., "3D Micro-tomographic Imaging and Quantitative Morphometry for the Nondestructive Evaluation of Porous Biomaterials," *Materials Research Society Symposium Proceedings*, Vol. 461, 1997, pp. 217-222.

[4] Garrido, L., "Non-destructive Evaluation of Synthetic Tissue Scaffolds with NMR", *Materials Research Society Symposium Proceedings*, Vol. 550, 1999, pp 171-176.

[5] Tjia, J. and Moghe, P., "Analysis of 3-D Microstructure of Porous Poly(lactide-glycolide) Matrices using Confocal Microscopy," *Journal of Biomedical Materials Research*, Vol. 43, No. 3, 1998, pp. 291-299.

[6] Birla, R. and Matthew, H. W. T., "3-Dimensional Imaging & Analysis of Smooth Muscle Colonization of Porous Chitosan Scaffolds," *Proceedings of the 1st Joint BMES/EMBS Conference*, 1999, p. 119.

[7] Drexler, W., Morganer, U., Kartner, F., Pitris, C., Boppart, S., Li, X., Ippen, E., and Fujimoto, J., "In vivo ultra-high resolution optical coherence tomography," *Optics Letters*, Vol. 24, No. 17, 1999, pp. 1221-1223.

[8] Wang, H.W., Izatt, J.A., and Kulkarni, D.D., "Optical Coherence Microscopy", *Handbook of Optical Coherence Tomography*, Bouma, B.E. and Tearney, G.J., Eds., Marcel Dekker, Inc. NewYork 2002, pp.275-298.

[9] Beaurepaire, E., Moreau, L., Amblard, F., Mertz, J., "Combined Scanning Optical Coherence and Two-Photon-Excited Fluorescence Microscopy", *Optics Letters*, Vol. 24, No.14, 1999, pp.969-971.

[10] Washburn, N., Simon, C., Tona, A., Elgendy, H., Karim, A. and Amis, E., "Co-extrusion of biocompatible polymers for scaffolds with co-continuous morphology," *Journal of Biomedical Materials Research*, Vol. 60, No. 1, 2002, pp. 20-29.